Comptes Rendus

Physique

Ralf Schützhold and William George Unruh

Space-time toy model for Hawking radiation

Research article / *Article de recherche*

Simulating gravitational problems with condensed matter analog models: a special issue in memory of Renaud Parentani (1962-2020) / *Simuler des problèmes gravitationnels avec des modèles analogues en matière condensée : un numéro spécial en mémoire de Renaud Parentani (1962-2020)*

Space-time toy model for Hawking radiation

Modèle-jouet spatio-temporel pour le rayonnement de Hawking

Ralf Schützhold [*, a, b] **and William George Unruh** [c, d]

[a] Helmholtz-Zentrum Dresden-Rossendorf, Bautzner Landstraße 400, 01328 Dresden, Germany

[b] Institut für Theoretische Physik, Technische Universität Dresden, 01062 Dresden, Germany

[c] Hagler Institute for Advanced Study, Institute for Quantum Science and Engineering, Texas A&M University, College Station, Texas 77843-4242, USA

[d] Department of Physics and Astronomy, University of British Columbia, Vancouver V6T 1Z1, Canada

E-mails: r.schuetzhold@hzdr.de (R. Schützhold), unruh@physics.ubc.ca (W. G. Unruh)

Abstract. By gluing together two sections of flat space-time in different metric representations (with the Minkowski metric representing the region far away from the black hole and the Rindler metric modeling the vicinity of the horizon), we construct a simplified toy model for black-hole evaporation. The simple structure of this toy model allows us to construct exact analytic solutions for the two-point functions in the various vacuum states (Israel–Hartle–Hawking, Unruh and Boulware states) in an easy way and thus helps to understand and disentangle the different ingredients for Hawking radiation better.

Résumé. En accolant deux sections de l'espace-temps plat en des représentations métriques différentes (la métrique de Minkowski représentant la région éloignée du trou noir et la métrique de Rindler modélisant le voisinage de l'horizon), nous construisons un modèle simplifié pour l'évaporation des trous noirs. La structure simple de ce modèle nous permet de construire facilement des solutions analytiques exactes pour les fonctions à deux points dans les différents états du vide (états Israel–Hartle–Hawking, Unruh et Boulware) et ainsi de mieux comprendre et démêler les différents ingrédients du rayonnement de Hawking.

Keywords. Black-hole evaporation, Energy–momentum tensor, Trace anomaly.

Mots-clés. Évaporation de trous noirs, Tenseur d'impulsion-énergie, Anomalie de trace.

*Corresponding author

1. Introduction

Hawking's striking discovery [1,2], predicting that black holes should evaporate by emitting thermal radiation with the temperature

$$\mathfrak{T}_{\text{Hawking}} = \frac{\hbar c^3}{8\pi k_{\text{B}} G_{\text{N}} M},\tag{1}$$

suggests deep links between gravity (G_{N}), relativity (c), quantum theory ($\hbar$) and thermodynamics (k_{B}). It seems as if nature is giving us a hint regarding its underlying structure. In order to interpret this hint correctly, it is important to properly understand the origin and mechanism of Hawking radiation. The curvature of space-time is sometimes identified as one of the reasons or even the reason for Hawking radiation. This idea could be supported by calculations [3] of the trace anomaly of the energy–momentum tensor where one observes that the space-time curvature can be interpreted as a source term in the energy–momentum balance law, see also Equation (11) below.

However, space-time curvature alone is not sufficient for predicting particle creation phenomena such as Hawking radiation. As a counter-example, one may consider the electromagnetic field around a neutron star in equilibrium which is described by a regular static metric. Unless there are photons incident from the outside, the electromagnetic field will quickly settle down to the local ground state in the vicinity of the star, and thus there is no lasting pair creation such as Hawking radiation. This is consistent with the trace anomaly calculation mentioned above, because a static metric and thus static curvature does not generate a source term in the balance law for energy—corresponding to the $v = 0$ component in Equation (11) below—but only a source term for the momentum balance (i.e., the $v = 1$ component) which can be interpreted as a force density.

Since the total energy is conserved in static or stationary space-times, lasting particle creation phenomena such as Hawking radiation are only possible if there is some place where the energy of the created particles comes from. For Hawking radiation, this is the horizon—the constant flux of positive energy out to infinity due to Hawking radiation (from the point of view of static observers far away) is compensated by the flux of negative energy into the horizon. However, this is still not the full picture since the quantum state near the horizon can be locally indistinguishable from vacuum while Hawking radiation is observed at infinity. Furthermore, the quantum energy inequalities (see, e.g., [4,5]) demand that the region with negative energy cannot be arbitrarily large (where the precise meaning of the term "arbitrarily large" depends on the explicit form of the inequality under consideration).

The transition, from the local vacuum near the horizon to the thermal radiation observed far away, is related to the space-time curvature, especially the spatial dependence of the red-shift. As a simplified intuitive picture, the finite pressure of the thermal radiation observed far away and the vanishing pressure of the local vacuum state near the horizon require some finite force density in between, which is generated by the curvature via the trace anomaly, see the $v = 1$ component of Equation (11) below.

Hence, Hawking radiation is caused by a combination of space-time curvature and the horizon. Since disentangling these effects is rather complicated for the Schwarzschild metric, we consider a simpler toy model in the following. To this end, we consider gluing together two regions

of flat space-time, one representing the vicinity of the horizon and the other one spatial infinity, such that the curvature is restricted to the boundary between the two regions. The fact that we have a piece-wise flat space-time simplifies the analysis and allows us to discuss the different vacuum states by means of exact analytic solutions.

2. The model

As motivated above, let us consider the following metric in $1+1$ dimensions ($\hbar = c = 1$)

$$\mathrm{d}s^2 = \begin{cases} e^{2\kappa x}(\mathrm{d}t^2 - \mathrm{d}x^2) & \text{for } x < 0 \\ \mathrm{d}t^2 - \mathrm{d}x^2 & \text{for } x > 0 \end{cases} \tag{2}$$

where κ corresponds to the surface gravity. For positive x, this metric just describes flat space-time in terms of the usual Minkowski coordinates t and x, while for for negative x, it is related to the Rindler metric $\mathrm{d}s^2 = \kappa^2 \rho^2 \mathrm{d}\tau^2 - \mathrm{d}\rho^2$ via the identification $t \leftrightarrow \tau$ and $x \leftrightarrow \rho_* = \ln(\kappa\rho)/\kappa$, i.e., the Regge–Wheeler tortoise coordinate.

In order to determine which part of the space-time is covered by these coordinates, we insert the inverse transformation $\rho = e^{\kappa \rho_*}/\kappa$ which maps the interval $\rho_* \in (-\infty, 0)$ to $\rho \in (0, 1/\kappa)$. Hence, the region of negative x corresponds to that part of the Rindler wedge where $0 < \rho < 1/\kappa$. Recalling the relations between Rindler τ, ρ and Minkowski coordinates T, X with $\mathrm{d}s^2 = \mathrm{d}T^2 - \mathrm{d}X^2$ which read $T = \rho \sinh(\kappa\tau)$ and $X = \rho \cosh(\kappa\tau)$, we see that both $x > 0$ and $x < 0$ correspond to flat space-time, though in different coordinates. At the boundary $x = 0$, however, we have an infinite curvature (which will become important below). Note that this boundary $x = 0$ is not the horizon, which is at $x \to -\infty$, i.e., $\rho = 0$. A visualization of the space-time (2) is given in Figure 1.

World-lines with constant $x > 0$ just describe static observers in Minkowski space-time whereas world-lines with constant $x < 0$ correspond to accelerated observers. On the other hand, inertial observers starting at $x < 0$ would either run to $x \to -\infty$ (i.e., reach the horizon) in a finite proper time or cross the boundary at $x = 0$. In that region $x > 0$, the world-lines of inertial observers are just the usual straight lines.

For the two-point functions discussed in the next section, it is advantageous to introduce the light-cone variables $u = t - x$ and $v = t + x$ such that

$$\mathrm{d}s^2 = \begin{cases} e^{\kappa(v-u)} \mathrm{d}u \, \mathrm{d}v & \text{for } v < u \\ \mathrm{d}u \, \mathrm{d}v & \text{for } v > u \end{cases}. \tag{3}$$

In the Rindler wedge, i.e., for $x < 0$, they are related to the standard Minkowski light-cone variables via $U = T - X = -e^{-\kappa u}/\kappa$ and $V = T + X = e^{\kappa v}/\kappa$ which gives $\mathrm{d}s^2 = \mathrm{d}U \, \mathrm{d}V$. Note that the coordinates T, X and U, V are regular across the horizon $\rho = 0$ and can be extended beyond it, see Figure 1.

3. Two-point functions

For simplicity, let us first consider a massless scalar field

$$\Box \phi = 0. \tag{4}$$

Due to its conformal invariance in $1+1$ dimensions, we get the usual decoupling into left- and right-moving modes

$$\phi(t, x) = \phi_{\text{left}}(t + x) + \phi_{\text{right}}(t - x) = \phi_{\text{left}}(v) + \phi_{\text{right}}(u). \tag{5}$$

After quantization, this decoupling into left- and right-moving modes does also apply to the quantum field, which facilitates the discussion of the different vacuum states.
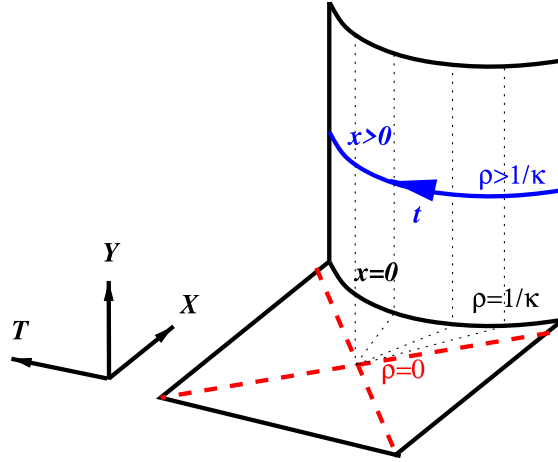
Figure 1. Visualization of the two-dimensional space-time (2) via an embedding into the three-dimensional Minkowski space-time $ds^2 = dT^2 - dX^2 - dY^2$. The horizontal plane corresponds to Minkowski space-time in terms of the coordinates T and X. The red dashed lines represent the coordinate lines $U = 0$ and $V = 0$ (i.e., $|X| = |T|$) which yield the future and past Rindler horizons at $\rho = 0$. The thin black dotted lines are coordinate lines where $t = $ const. The region between the Rindler horizons at $\rho = 0$ and the hyperbola $\rho = 1/\kappa$ (which corresponds to an accelerated trajectory in terms of the coordinates T and X) is covered by the coordinates (2) for $x < 0$. The remaining section of Minkowski space-time for $x > 0$ is represented by the vertical sheet which displays extrinsic but no intrinsic curvature. The two parts $x < 0$ and $x > 0$ are glued together at $x = 0$, i.e., $\rho = 1/\kappa$. Each part is locally flat, i.e., could be "ironed" to a planar surface. However, after gluing them together, this is no longer possible—which reflects the curvature singularity at $x = 0$.

3.1. *Israel–Hartle–Hawking vacuum*

Casting aside the problems related to the infrared divergence of the massless scalar field in $1+1$ dimensions for a moment, the Minkowski vacuum in the Rindler wedge (for $x < 0$) has the standard two-point function (away from the light cone)

$$\langle \hat{\phi}(t, x<0) \hat{\phi}(t', x'<0) \rangle = -\frac{1}{4\pi} \ln[\kappa^2 \Delta U \Delta V] = -\frac{1}{4\pi} \ln[\kappa^2(T-T')^2 - \kappa^2(X-X')^2]$$

$$= -\frac{1}{4\pi} \ln[2e^{\kappa(x+x')} \cosh(\kappa[t-t']) - e^{2\kappa x} - e^{2\kappa x'}], \tag{6}$$

where $\Delta U = U - U'$ and $\Delta V = V - V'$. Now, since this two-point function is a solution of the wave equation $(\partial_t^2 - \partial_x^2)\phi = 0$ for both arguments t, x and t', x' and all values of x and x', it has the same form—in terms of the coordinates t, x and t', x'—on the other side $x > 0$ where it describes a thermal state with the Unruh temperature $\mathfrak{T}_{\text{Unruh}} = \kappa/(2\pi)$. Hence, this state corresponds to the Israel–Hartle–Hawking state [6,7].

3.2. *Boulware vacuum*

In contrast, let us start from the Minkowski vacuum in the other region $x > 0$

$$\langle \hat{\phi}(t, x>0) \hat{\phi}(t', x'>0) \rangle = -\frac{1}{4\pi} \ln[\kappa^2 \Delta u \Delta v] = -\frac{1}{4\pi} \ln[\kappa^2(t-t')^2 - \kappa^2(x-x')^2]. \tag{7}$$

With the same argument as before, this form remains correct in the Rindler wedge, i.e., for $x < 0$, where it corresponds to the Rindler vacuum. This state is the ground state of the Hamiltonian generating the time t evolution, which is usually referred to as the Boulware vacuum [8]. In contrast to the Israel–Hartle–Hawking state above, this state becomes singular in terms of the T and X coordinates when approaching the horizon at $x \to -\infty$.

3.3. *Unruh vacuum*

For a state corresponding to black-hole evaporation [9], we take the left-moving modes to start in the Minkowski vacuum at $x > 0$, given by the v-term in Equation (7), while the right-moving modes start in the Minkowski vacuum at $x < 0$, given by the u-contribution in Equation (6)

$$\langle \hat{\phi}(t, x) \hat{\phi}(t', x') \rangle = -\frac{1}{4\pi} (\ln[\kappa \Delta U] + \ln[\kappa \Delta v]) = -\frac{1}{4\pi} (\ln[e^{-\kappa u'} - e^{-\kappa u}] + \ln[\kappa \Delta v]). \tag{8}$$

Since the right-moving modes start in the Minkowski vacuum at $x < 0$, they are regular at the horizon. After propagating to the other side $x > 0$, inertial observers perceive them as thermal radiation. The same inertial observers at $x > 0$ would assign zero occupation numbers to the left-moving modes. However, after the left-moving modes propagate to the other side $x < 0$, they would no longer appear unoccupied for inertial observers. In fact, similar to the Rindler vacuum state, they would become singular at the (past) horizon.

4. Energy–momentum tensor

After having discussed the two-point functions, let us investigate the renormalized expectation value of the energy–momentum tensor $\langle \hat{T}^\mu_\nu \rangle_{\text{ren}}$. In principle, this quantity $\langle \hat{T}^\mu_\nu \rangle_{\text{ren}}$ can be obtained via the point-slitting technique from the above two-point functions (or other techniques). Here, we employ energy balance law $\nabla_\mu \langle \hat{T}^\mu_\nu \rangle_{\text{ren}} = 0$ which can be cast into the form

$$\frac{1}{\sqrt{-g}} \partial_\mu \left(\sqrt{-g} \langle \hat{T}^\mu_\nu \rangle_{\text{ren}} \right) = \frac{1}{2} \langle \hat{T}^{\alpha\beta} \rangle_{\text{ren}} \partial_\nu g_{\alpha\beta}. \tag{9}$$

For the metric (2), the right-hand side is proportional to the trace $\langle \hat{T}^\mu_\mu \rangle_{\text{ren}}$. For the classical field (4), this trace would be zero, but quantum fields in curved space-times acquire a trace anomaly [3], which is, for the massless scalar field, given by $\langle \hat{T}^\mu_\mu \rangle_{\text{ren}} = R/(24\pi)$ in terms of the Ricci scalar R.

For $x \neq 0$, the metric (2) just corresponds to flat space-time and thus does not have any curvature, but at $x = 0$, we get a delta singularity in R and thus $\langle \hat{T}^\mu_\mu \rangle_{\text{ren}}$ which can be interpreted as a source term in Equation (9). Note that special care is required for computing this source term as the delta function in $\langle \hat{T}^\mu_\mu \rangle_{\text{ren}}$ is multiplied with the metric derivative $\partial_\nu g_{\alpha\beta}$ which has a Heaviside like step at $x = 0$. One way would be to start with a smooth metric and then take the appropriate limit, another option would be to split off the trace term and consider the trace-free part $\theta_{\mu\nu}$, see Section 4.4 below.

However, symmetry arguments already allow us to draw some general conclusions at this stage: Since the metric (2) is static and $\langle \hat{T}^\mu_\nu \rangle_{\text{ren}}$ is stationary for the three vacuum states discussed above, all time-derivatives ∂_t vanish in Equation (9). Then, evaluating Equation (9) for $\nu = 0$, we find that the normalized energy flux $\sqrt{-g} \langle \hat{T}^1_0 \rangle_{\text{ren}}$ (or momentum density) must always be constant across the whole space-time. For $\nu = 1$, Equation (9) allows us to determine the effective pressure $\sqrt{-g} \langle \hat{T}^1_1 \rangle_{\text{ren}}$. The spatial derivative of the metric (2) vanishes for $x > 0$ and reads $\partial_x g_{\alpha\beta} = 2\kappa g_{\alpha\beta}$ for $x < 0$. Thus, the effective source term on the right-hand side of Equation (9) vanishes identically for $x > 0$ and equals the trace $\langle \hat{T}^\mu_\mu \rangle_{\text{ren}}$ multiplied by κ for $x < 0$. However, since this trace is, in our simplified metric (2), zero for $x < 0$, we find that the right-hand side of
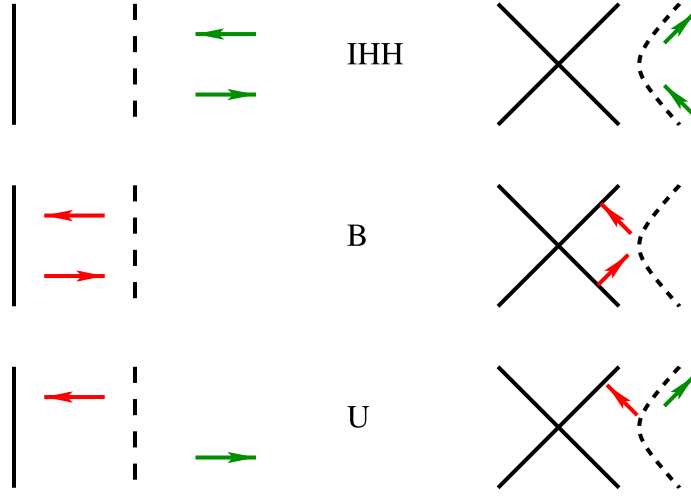
Figure 2. Sketch of the fluxes in the Israel–Hartle–Hawking (top), Boulware (middle) and Unruh (bottom) vacua in space-time diagrams using the Rindler τ, ρ coordinates (left) and the Minkowski T, X coordinates (right). Red arrows denote flux of negative energy while green arrows correspond to positive energy. The solid black lines represent the Rindler horizon(s) at $\rho = 0$ while the dashed line marks the gluing line at $\rho = 1/\kappa$.

Equation (9) vanishes both for $x > 0$ and for $x < 0$. As a result, the effective pressure $\sqrt{-g}\,\langle \hat{T}_1^1 \rangle_{\text{ren}}$ is piece-wise constant for $x > 0$ and for $x < 0$ with a jump or step at $x = 0$. Again using that the trace $\langle \hat{T}_\mu^\mu \rangle_{\text{ren}}$ vanishes for $x \neq 0$, we may infer that the energy density $\sqrt{-g}\,\langle \hat{T}_0^0 \rangle_{\text{ren}}$ behaves in the same way, i.e., it is piece-wise constant for $x > 0$ and for $x < 0$ but displays a jump or step at $x = 0$. Note, however, that the singularity structures of $\sqrt{-g}\,\langle \hat{T}_1^1 \rangle_{\text{ren}}$ and $\sqrt{-g}\,\langle \hat{T}_0^0 \rangle_{\text{ren}}$ at $x = 0$ may differ.

4.1. *Israel–Hartle–Hawking vacuum*

Since the Israel–Hartle–Hawking vacuum just corresponds to the Minkowski vacuum for $x < 0$, we have $\langle \hat{T}_\nu^\mu \rangle_{\text{ren}} = 0$ in this region $x < 0$. With the argument above, this already implies that the energy flux vanishes everywhere $\langle \hat{T}_0^1 \rangle_{\text{ren}} = 0$. This should be no surprise because for $x > 0$ the Israel–Hartle–Hawking vacuum is indistinguishable from a thermal state with the Unruh temperature where the left- and right-moving fluxes cancel each other, as indicated in Figure 2. In this thermal region $x > 0$, we find the usual energy density of a thermal bath $\langle \hat{T}_0^0 \rangle_{\text{ren}} \propto \kappa^2$. Thus energy density and pressure are positive for $x > 0$ and jump to zero at $x = 0$ where the jump in pressure is counter-balanced by the curvature singularity.

4.2. *Boulware vacuum*

When going from the Israel–Hartle–Hawking state to the Boulware vacuum, we have to subtract the thermal bath of particles. For $x > 0$, this just means that $\langle \hat{T}_\nu^\mu \rangle_{\text{ren}}$ is reduced to zero—as expected in the Minkowski vacuum. On the other side $x < 0$, however, this subtraction implies that the energy density $\langle \hat{T}_0^0 \rangle_{\text{ren}}$ must become negative: Here world-lines with constant x correspond to uniformly accelerated observers who would experience the Minkowski vacuum (i.e., the Israel–Hartle–Hawking state discussed above) as a thermal bath of particles. From the point of view of those Rindler observers, the energy density $\langle \hat{T}_0^0 \rangle_{\text{ren}}$ can be split up into two

parts—the energy density of the Rindler vacuum and the energy density from the thermal bath of particles. The latter is always positive and thus removing it yields a negative energy density for the Rindler vacuum since we started from $\langle \hat{T}^\mu_\nu \rangle_{\text{ren}} = 0$ in the Minkowski vacuum, cf. Figure 2. Hence, the energy density and pressure make the same step as before, but are globally shifted down. As before, the normalized energy flux must vanish everywhere since $\langle \hat{T}^\mu_\nu \rangle_{\text{ren}}$ is zero for $x > 0$.

4.3. *Unruh vacuum*

A non-vanishing flux is obtained in the Unruh state where the incoming (i.e., left-moving) modes are in their vacuum state for $x > 0$ while the outgoing (i.e., right-moving) modes are thermally occupied for $x > 0$. This results in a flux of positive energy moving out to $x \to \infty$. Since $\sqrt{-g} \langle \hat{T}^1_0 \rangle_{\text{ren}}$ must be the same for all x, we also find an energy flux for $x < 0$. From the point of view of the Rindler observers (at constant and negative x), the left-moving modes are in the Rindler vacuum state (i.e., unoccupied by particles) while the right-moving modes are thermally occupied, cf. Figure 2. These thermal particles compensate the negative energy density of the Rindler vacuum itself for the right-moving modes, but they are absent for the left-moving modes, which means that we have a flux of negative energy to $x \to -\infty$.

4.4. *Trace-free tensor*

As already mentioned above, an alternative way of interpreting the results is to define a trace-free tensor $\theta_{\mu\nu}$ by splitting off the trace anomaly [3]

$$\langle \hat{T}_{\mu\nu} \rangle_{\text{ren}} = \theta_{\mu\nu} + \frac{R}{48\pi} g_{\mu\nu}, \tag{10}$$

such that $\theta^\mu_\mu = 0$. In terms of $\theta_{\mu\nu}$, the energy balance law $\nabla_\mu \langle \hat{T}^\mu_\nu \rangle_{\text{ren}} = 0$ becomes

$$\nabla_\mu \theta^\mu_\nu = \frac{1}{\sqrt{-g}} \partial_\mu (\sqrt{-g}\, \theta^\mu_\nu) = -\frac{\partial_\nu R}{48\pi}, \tag{11}$$

where the role of the curvature as the source term becomes even more apparent. For a metric of the form $ds^2 = C(u,v)\, du\, dv$ such as in Equation (2), point-splitting renormalization yields the following result

$$\theta_{uu} = -\frac{\sqrt{C}}{12\pi} \frac{\partial^2}{\partial u^2} \frac{1}{\sqrt{C}}, \quad \theta_{vv} = -\frac{\sqrt{C}}{12\pi} \frac{\partial^2}{\partial v^2} \frac{1}{\sqrt{C}}, \quad \theta_{uv} = \theta_{vu} = 0, \tag{12}$$

for the vacuum state corresponding to the u and v coordinates, which is the Boulware vacuum state in our case.

Inserting the metric in Equations (2) and (3), we find that $\theta_{\mu\nu}$ vanishes for $x > 0$ as expected. For $x < 0$, on the other hand, we find the constant values $\theta_{uu} = \theta_{vv} = -\kappa^2/(48\pi)$. Apart from the jump at $x = 0$, these terms do also contain delta singularities at $x = 0$.

For the Israel–Hartle–Hawking vacuum, this negative energy density in the $x < 0$ region is shifted up to zero by adding a constant to the energy density $\sqrt{-g} \langle \hat{T}^0_0 \rangle_{\text{ren}}$ (in terms of the original t and x coordinates) such that we arrive at a positive energy density for $x > 0$.

For the Unruh vacuum, this shift only applies to the right-moving modes, while the left-moving modes remain unaffected. As a result, we only obtain half the energy density for $x > 0$ in comparison to the Israel–Hartle–Hawking vacuum. Furthermore, this asymmetry between left- and right-moving modes induces a non-zero energy flux, as discussed above.

5. Potential barrier

So far, we considered the case of a massless scalar field in $1+1$ dimensions, which is conformally invariant. As a result, the left- and right-moving modes decouple—which greatly simplifies the analysis. In the general case, however, the conformal invariance is broken, e.g., by a finite mass term, fields with higher spin, or the angular barrier in $3+1$ dimensions. These effects typically induce back-scattering, i.e., the scattering from left- to right-moving modes and vice versa.

In order to incorporate back-scattering into our toy model, we introduce an additional delta potential at $x = 0$

$$\Box \phi = \gamma \delta(x) \phi. \tag{13}$$

In terms of the usual mode decomposition for the initial quantum fields

$$\hat{\phi}_{\text{left}}^{\text{in}} = \int d\omega \, \frac{e^{-i\omega(t+x)}}{\sqrt{4\pi\omega}} \, \hat{a}_{\omega}^{\text{left}} + \text{h.c.}, \quad \hat{\phi}_{\text{right}}^{\text{in}} = \int d\omega \, \frac{e^{-i\omega(t-x)}}{\sqrt{4\pi\omega}} \, \hat{a}_{\omega}^{\text{right}} + \text{h.c.}, \tag{14}$$

the potential barrier then induces the reflection and transmission coefficients

$$\hat{a}_{\omega}^{\text{left}} \to \mathcal{T}_{\omega} \hat{a}_{\omega}^{\text{left}} + \mathcal{R}_{\omega} \hat{a}_{\omega}^{\text{right}}, \quad \hat{a}_{\omega}^{\text{right}} \to \mathcal{T}_{\omega}^{*} \hat{a}_{\omega}^{\text{right}} + \mathcal{R}_{\omega}^{*} \hat{a}_{\omega}^{\text{left}}, \tag{15}$$

with $1/\mathcal{T}_{\omega} = i\gamma/(2\omega) + 1$ and $1/\mathcal{R}_{\omega} = 2i\omega/\gamma - 1$ for the simple delta potential (13), but other potentials can be treated in complete analogy.

This allows us to calculate all expectation values for the final modes in terms of expectation values of the initial operators $\hat{a}_{\omega}^{\text{left}}$ and $\hat{a}_{\omega}^{\text{right}}$ such as

$$\langle (\hat{a}_{\omega}^{\text{left}})^{\dagger} \hat{a}_{\omega}^{\text{left}} \rangle \to |\mathcal{T}_{\omega}^{2}| \langle (\hat{a}_{\omega}^{\text{left}})^{\dagger} \hat{a}_{\omega}^{\text{left}} \rangle + |\mathcal{R}_{\omega}^{2}| \langle (\hat{a}_{\omega}^{\text{right}})^{\dagger} \hat{a}_{\omega}^{\text{right}} \rangle + [\mathcal{T}_{\omega}^{*} \mathcal{R}_{\omega} \langle (\hat{a}_{\omega}^{\text{left}})^{\dagger} \hat{a}_{\omega}^{\text{right}} \rangle + \text{h.c.}]. \tag{16}$$

In the cases considered here, the initial modes incident from left and right are uncorrelated such that the mixed terms in the square bracket on the right-hand side vanish. For the Boulware and the Israel–Hartle–Hawking states, the two expectation values $\langle (\hat{a}_{\omega}^{\text{left}})^{\dagger} \hat{a}_{\omega}^{\text{left}} \rangle$ and $\langle (\hat{a}_{\omega}^{\text{right}})^{\dagger} \hat{a}_{\omega}^{\text{right}} \rangle$ give the same result—in the first case, both vanish and in the second case, both yield the same thermal distribution. Together with unitarity $|\mathcal{T}_{\omega}^{2}| + |\mathcal{R}_{\omega}^{2}| = 1$, we find that all local expectation values (or, more generally, all expectation values confined to one side) yield the same results as in the case without the potential. In contrast, correlations between the two sides will be generated by the potential.

In the Unruh vacuum, however, the two expectation values differ: $\langle (\hat{a}_{\omega}^{\text{left}})^{\dagger} \hat{a}_{\omega}^{\text{left}} \rangle$ vanishes while $\langle (\hat{a}_{\omega}^{\text{right}})^{\dagger} \hat{a}_{\omega}^{\text{right}} \rangle$ yields a thermal distribution. Thus the positive energy flux going out to $x \to \infty$ will be reduced by the gray-body factor $|\mathcal{T}_{\omega}^{2}| \langle (\hat{a}_{\omega}^{\text{right}})^{\dagger} \hat{a}_{\omega}^{\text{right}} \rangle$ while the flux of negative energy to $x \to -\infty$ is partially compensated by the reflected thermal radiation $|\mathcal{R}_{\omega}^{2}| \langle (\hat{a}_{\omega}^{\text{right}})^{\dagger} \hat{a}_{\omega}^{\text{right}} \rangle$.

As an intuitive picture, one can say that the negative flux of energy into the horizon is created by the absence of the particles which would be flowing into the black hole in the Israel–Hartle–Hawking state. The escape of particles to $x \to \infty$ instead of their reflection back into the future horizon creates that negative flux.

6. Conclusions and outlook

For a better understanding of complex phenomena in Nature, it is often useful to construct suitable toy models (see, e.g., [10]) which reproduce essential features of the original phenomenon. Here, we consider the phenomenon of Hawking radiation, i.e., black-hole evaporation[1]. In order to disentangle the roles played by space-time curvature and horizon, we construct a toy model

---

[1] The conclusions of this paper were also presented in General Relativity and Gravitation [11].

by gluing together[2] two patches of piece-wise flat space-times in Rindler and Minkowski coordinates, see Figure 1. This simplified space-time allows us to provide compact analytic solutions for the two-point functions and the energy–momentum tensor for the Israel–Hartle–Hawking, Unruh and Boulware vacua, see Figure 2.

In the Unruh and Boulware vacua, we find a negative energy density in the Rindler patch, which can be explained by the absence of Rindler particles which would lift the energy density up to zero in the Israel–Hartle–Hawking vacuum (which is just the Minkowski vacuum inside this Rindler patch). Note that, consistent with the energy inequalities, inertial observers cannot stay forever in the Rindler patch, they either fall into the black hole or move out to the Minkowski patch in a finite proper time.

In order to mimic the curvature potential of black holes, we also considered a potential barrier in the form of a simple delta potential. For Israel–Hartle–Hawking and Boulware vacua, this additional potential does not change the particle spectra (only the correlations between different sides of the delta potential change). For the Unruh vacuum, on the other hand, we find a gray-body factor for the outgoing radiation, as expected.

Instead of the most simple example of a scalar field considered here, one could generalize our studies to massless fermions in $1 + 1$ dimensions, see, e.g., [15–18]. There are two main differences. First, the total flux is obtained by an integral over the Fermi–Dirac distribution (with $\exp\{\omega/(k_{\mathrm{B}}\mathfrak{T}_{\mathrm{Hawking}})\}+1$ in the denominator) instead of the Bose–Einstein (or Planck) distribution (with $\exp\{\omega/(k_{\mathrm{B}}\mathfrak{T}_{\mathrm{Hawking}})\}-1$ in the denominator), which yields a reduction by a factor of two. Second, we have to sum over more species in the fermionic case. On the one hand, particles and anti-particles both contribute equally to the total flux (as would also happen for a complex scalar field) and, on the other hand, we have to add up the spin species (depending on the realization, e.g., 2×2 or 4×4 Dirac matrices). Nevertheless, up to the resulting pre-factor, we obtain the same result for trace anomaly. Thus, the qualitative results for energy density and flux as well as pressure for the three vacuum states under consideration should be equivalent.

Declaration of interests

The authors do not work for, advise, own shares in, or receive funds from any organization that could benefit from this article, and have declared no affiliations other than their research organizations.

Funding

---

[2]A similar idea of gluing together such space-times has been pursued in [12], see also [13] and [14]. However, there are important differences to our scenario. By gluing at a fixed position $x = 0$, we obtain a static space-time (2). In contrast, the "Rindler quench" considered in [12] implies gluing at a fixed time, such that the resulting space-time is time-dependent. As a result, in spite of some similarities, the underlying mechanisms for pair creation are different.

Acknowledgments

References

[1]   S. W. Hawking, "Particle creation by black holes", *Commun. Math. Phys.* **43** (1975), pp. 199–220. [erratum: Commun. Math. Phys. **46**, 206 (1976)].

[2]   S. W. Hawking, "Black hole explosions", *Nature* **248** (1974), pp. 30–31.

[3]   P. C. W. Davies, S. A. Fulling and W. G. Unruh, "Energy momentum tensor near an evaporating black hole", *Phys. Rev. D* **13** (1976), pp. 2720–2723.

[4]   C. J. Fewster, "Lectures on quantum energy inequalities", Preprint, 1208.5399.

[5]   L. H. Ford and T. A. Roman, "Averaged energy conditions and quantum inequalities", *Phys. Rev. D* **51** (1995), pp. 4277–4286.

[6]   W. Israel, "Thermo field dynamics of black holes", *Phys. Lett. A* **57** (1976), pp. 107–110.

[7]   J. B. Hartle and S. W. Hawking, "Path integral derivation of black hole radiance", *Phys. Rev. D* **13** (1976), pp. 2188–2203.

[8]   D. G. Boulware, "Quantum field theory in Schwarzschild and Rindler spaces", *Phys. Rev. D* **11** (1975), pp. 1404–1423.

[9]   W. G. Unruh, "Notes on black hole evaporation", *Phys. Rev. D* **14** (1976), pp. 870–892.

[10]   C. Maia and R. Schützhold, "Quantum toy model for black-hole back-reaction", *Phys. Rev. D* **76** (2007), article no. 101502.

[11]   W. G. Unruh, "Black hole evaporation – 50 years", *Gen. Relativ. Gravit.* **57** (2025), article no. 78.

[12]   J. Louko, "Thermality from a Rindler quench", *Class. Quant. Grav.* **35** (2018), no. 20, article no. 205006.

[13]   J. Rodriguez-Laguna, L. Tarruell, M. Lewenstein and A. Celi, "Synthetic Unruh effect in cold atoms", *Phys. Rev. A* **95** (2017), no. 1, article no. 013627.

[14]   R. Schützhold, "On the Hawking effect", *Phys. Rev. D* **64** (2001), article no. 024029.

[15]   P. C. W. Davies and W. G. Unruh, "Neutrino stress tensor regularization in two-dimensional space-time", *Proc. Roy. Soc. Lond. A* **356** (1977), pp. 259–268.

[16]   B. S. DeWitt, "The global approach to quantum field theory. Vol. 1, 2", *Int. Ser. Monogr. Phys.* **114** (2003), pp. 1–1042.

[17]   S. M. Christensen, "Regularization, renormalization, and covariant geodesic point separation", *Phys. Rev. D* **17** (1978), pp. 946–963.

[18]   R. Ferrero, S. A. Franchino-Viñas, M. B. Fröb and W. C. C. Lima, "Universal definition of the nonconformal trace anomaly", *Phys. Rev. Lett.* **132** (2024), no. 7, article no. 071601.